Int. J. Heat Mass Transfer. Vol. 33, No. 9, pp. 1839–1847, 1990
Printed in Great Britain

0017-9310/90 $3.00 + 0.00

Response of a solid–gas growth interface to an increase in temperature

BERNARD ZAPPOLI and DIDIER BAILLY
Centre National d'Etudies Spatiales, 18, Avenue E. Belin, 31055 Toulouse Cédex, France

(*Received* 8 *February* 1989 *and in final form* 9 *October* 1989)

Abstract—Transient crystal growth from a vapour phase in micro-gravity conditions is studied through a one-dimensional model problem. This model consists of solving by means of the PISO algorithm the full continuity, momentum, energy and transport equation of the specie which reacts at the interface in order to explore the transient between two states of equilibrium of a crystal with its vapour at two different temperatures. Solution of the governing equations is also obtained using a matched asymptotic expansion technique and comparison with the numerical results of Part I concerning the evolution on the acoustic time is a good validation of the numerical method and scaling laws.

1. INTRODUCTION

DUE TO the strong decrease of buoyant convection, second-order forces may drive significant fluid flows in micro-gravity conditions. In liquids, the Marangoni effect which has its origin in the interface force caused by a surface tension gradient is a well-known example of second-order motion which has been extensively studied. In gases, the compressibility may generate motion even in the absence of buoyant forces. It is well known, for example, that when heat is added to the wall of a closed vessel, a motion is generated in the fluid in the form of acoustic waves, and depending on the time rate and the amount of heat addition you can even generate shock waves [1, 2].

The physical problem under study is the following: a crystal, located on the wall of a one-dimensional slot filled with a binary perfect gas mixture is in equilibrium with this mixture one component of which is the gaseous phase of the crystal. The system is in quasi zero-gravity conditions. For $t = 0$ the crystal is heated until it reaches a new temperature; as the slot is closed and insulated, a new thermodynamic equilibrium is reached and the aim of this paper is to explore the transient between these two equilibria.

In the first part, a slow heating law is considered, that is to say the temperature of the crystal is raised on the long diffusive time scale. The solution of the Navier–Stokes equations is looked for under the form of an asymptotic expansion written for the short acoustic time scale. In a similar way as in ref. [3], the matched asymptotic expansion technique is used to match the initial boundary layer with the core flow. Then the multiple scale expansion technique is used to obtain the equations which describe the evolution on the long diffusive time scale.

The second part is the numerical solution of the problem by the PISO algorithm [4]. After the principle of the method is given, solution for the same boundary conditions as in Part I is obtained for comparison of the results. A typical evolution is then computed on both acoustic and diffusive time scales in the boundary layer and core flow.

2. THE ASYMPTOTIC ANALYSIS

2.1. *The Physical Situation*

The physical problem concerns a confined, two-component perfect gas mixture contained in a one-dimensional slot of width L situated in micro-gravity conditions. At the end located at $x = 0$ a crystal is at the thermodynamic equilibrium at the initial temperature and pressure T_0 and P_0. The other end, $x = 1$, is closed and insulated. For $t = 0$ the temperature at $x = 0$ is raised on a long time scale until it reaches a new temperature; after a transient, a new equilibrium of the crystal with its vapour is reached for which the thermodynamic properties are constant and the fluid is at rest. This problem is an extension of the one studied in ref. [3] for which there is no growth interface.

2.2. *The Governing Equations*

The governing equations are the Navier–Stokes equations coupled with the diffusion equation of the specie which reacts at the interface at $x = 0$. If the length x', velocity u' and time are respectively reported to the length L of the medium, the sound velocity C'_0 and the acoustic time $t'_a = L/C'_0$ while the temperature T', the pressure P' and the specific mass are normalized with respect to their initial values, the governing equations can be written as follows:

continuity

$$\rho_t + (\rho u)_x = 0; \tag{1}$$

NOMENCLATURE

C'_0	sound velocity in the initial reference state
D	diffusion coefficient
L	width of the slot
Le	Lewis number
M_x	molar mass of specie x
P	pressure
Pr	Prandtl number
t'_a	acoustic characteristic time
t'_d	diffusive characteristic time
t	time normalized with respect to the acoustic characteristic time
T	temperature
T_0	reference initial temperature
W	weight fraction for specie A
W_0	initial value for the weight fraction of A
x	space variable
z	inner space variable.

Greek symbols

α^{-1}	molar mass of the mixture
δ	boundary layer thickness
ε	small parameter
κ	thermal diffusivity
ρ	specific mass of the bulk gaseous phase
ρ_0	initial value of the specific mass
ρ'^{e}_A	equilibrium value of the partial specific mass of A at the interface
τ	time normalized with respect to the diffusive characteristic time.

Superscripts and subscripts

$(\ )'$	dimensional variable
$(\bar{\ })$	outer variable
$(\tilde{\ })$	inner variable
$(\ )_A$	property related to specie A

momentum

$$\rho u_t + \rho u u_x = -\gamma^{-1} P_x + \tfrac{4}{3}\varepsilon u_{xx}; \qquad (2)$$

energy

$$\frac{\rho}{\gamma-1}(T_t + uT_x) = -Pu_x + \varepsilon\left\{\frac{\gamma}{\gamma-1} Pr^{-1} T_{xx} + \tfrac{4}{3}\gamma(u_x)^2\right\}; \qquad (3)$$

species

$$W_t + \left(u - \frac{\varepsilon}{Pr\,Le}\frac{\rho_x}{\rho}\right)W_x = \frac{\varepsilon}{Pr\,Le} W_{xx} \qquad (4)$$

where W is the weight fraction and the pressure is given by

$$P = \rho\alpha T$$

where

$$\alpha = \frac{\alpha'}{\alpha'_0}; \quad \alpha' = \frac{M_B - M_A}{M_A M_B} W + \frac{1}{M_B} = k_1 W + k_2.$$

M_A and M_B are respectively the molar masses of the reacting component at the interface and that of the inert one B. ε is the ratio $Pr\, t'_a/t'_d$ of the acoustic time t'_a to the diffusion time $t'_d = L^2/\kappa$ where κ is the thermal diffusivity. γ is the ratio of specific heats.

2.2.1. *Boundary conditions*

2.2.1.1. *Boundary conditions at* $x = 0$.

$$T = H(\tau) = H(\varepsilon t) = 1 + H'(0)\varepsilon t + O(\varepsilon^2) \qquad (5)$$

where τ is the time normalized with respect to the diffusion time

$$\tau = \varepsilon t.$$

Equation (5) means that the heating of the crystal occurs on the long diffusive scale. Typically, for air at STP and $L = 0.1$ m the following numerical values hold:

$$t'_a = 3\times10^{-4}\,\text{s}; \quad C'_0 = 3\times10^2\,\text{m s}^{-1}; \quad t'_d = 6.29\times10^2\,\text{s}.$$

Now, if the phase change reaction which takes place at $x = 0$ is supposed to be extremely rapid compared to diffusion in the bulk, then the mass transfer at the interface is diffusion limited and the weight fraction at this interface is thus fixed to its equilibrium value [5]

$$\rho'_A = \rho'^{e}_A(T) \quad \text{or} \quad W = \frac{W^e_A(T)}{\rho} \quad \text{at} \quad x = 0$$

where $W^e_A(T)$ is the equilibrium weight fraction when the partial specific mass of A is reported to the initial specific mass ρ'_0.

Taking into account equation (5), the equilibrium weight fraction at the interface may be expanded as

$$\rho W = W_0 + \varepsilon G'(1)H'(0)t + O(\varepsilon^2) \qquad (6)$$

where

$$G'(1) = \left.\frac{\partial W}{\partial T}\right|_{T=1}$$

and the boundary condition for the velocity at $x = 0$ is deduced from the mass balance [5]

$$u = \frac{\varepsilon}{Pr\,Le}\frac{W_x}{\dfrac{W}{\rho} - 1} \quad \text{at} \quad x = 0. \qquad (7)$$

2.2.1.2. *Boundary conditions at* $x = 1$. The slot is closed at $x = 1$ and insulated, so that

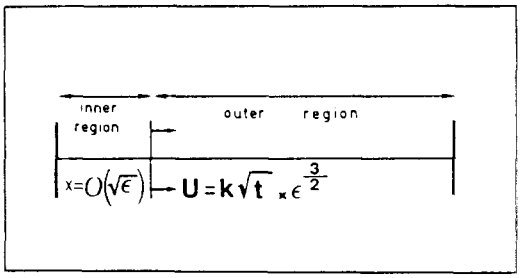

FIG. 1. Asymptotic analysis on the acoustic time scale.

$$u = 0; \quad T_x = 0, \quad W_x = 0. \tag{8}$$

2.2.1.3. *Initial conditions.*

$$\rho = T = P = 1, \quad u = 0, \quad W = W_0 \quad \text{at} \quad t = 0. \tag{8'}$$

2.3. *Asymptotic Solution on the Acoustic Time Scale*

The main scaling and domain defined in this analysis are summarized on Fig. 1.

2.3.1. *Initial boundary layer solution (inner solution)*

2.3.1.1. *The solution.* From equation (4) and boundary conditions (5) it is clear that the asymptotic expansion

$$T = 1 + \varepsilon \tilde{T}(x, t) + o(\varepsilon)$$

is not regular in the neighbourhood of $x = 0$ and that ε is a singular perturbation parameter for $x = 0$. According to the matched asymptotic expansion technique, an inner variable defined by

$$z = \frac{x}{\delta(\varepsilon)}, \quad \delta(\varepsilon) \to 0 \quad \text{as} \quad \varepsilon \to 0 \tag{9}$$

must be introduced and the solution seeked under the form of another asymptotic expansion called the inner expansion and constructed for the function

$$T(\delta z, t) = \tilde{T}(z, t)$$

that is to say

$$T = 1 + \varepsilon \tilde{T}(z, t) + o(\varepsilon). \tag{10}$$

The function $\delta(\varepsilon)$ is given by the least degeneracy principle which matches the transient and diffusion terms in equation (4) written for the function $\tilde{T}(z, t)$ and for the inner variable z. This gives obviously

$$\delta(\varepsilon) = \sqrt{\varepsilon}. \tag{11}$$

Physically this means that the heat diffusion has no time to occur on the short acoustic time scale except in a very thin layer of thickness ε just in front of the heated crystal. In the same way a species diffusion boundary layer is formed.

The scaling for the other variables in this layer, that is to say the definition of the compatible asymptotic sequence for the inner expansion, is given by matching the linear terms [3] in each equation when ρ, P and u are expanded as

$$\rho = 1 + \varepsilon^{\alpha} \tilde{\rho} + o(\varepsilon^{\alpha}) \tag{12}$$

$$P = 1 + \varepsilon^{\pi} \tilde{P} + o(\varepsilon^{\pi}) \tag{13}$$

$$u = \varepsilon^{\beta} \tilde{u} + o(\varepsilon^{\beta}) \tag{14}$$

which gives

$$\alpha = 1; \quad \beta = \tfrac{3}{2} \quad \text{and} \quad \pi = 2. \tag{15}$$

Considering equation (6) the scaling for W in the boundary layer is

$$W = W_0 + \varepsilon \tilde{W}(z, t) + o(\varepsilon). \tag{16}$$

Substituting equations (16) and (11) in boundary condition (7) for u gives

$$\tilde{u}(z = 0, t) = O(\varepsilon^{3/2})$$

which means that the mass transport is of the same order as the thermal effects in the compressible boundary layer.

Substituting equations (10)–(16) for T, x, ρ, P and W in equations (1)–(4) the following governing equations are obtained for the first-order approximation in the boundary layer:

$$\tilde{\rho}_t + \tilde{u}_z = 0 \tag{17}$$

$$\tilde{\rho} + \tilde{T} = \frac{k_1}{k_1 W_0 + k_2} \tilde{W} = -\xi \tilde{W} \tag{18}$$

$$\tilde{T}_t = -(\gamma - 1)\tilde{u}_z + \gamma \, Pr^{-1} \tilde{T}_{zz} \tag{19}$$

$$\tilde{u}_t = -\gamma^{-1} \tilde{P}_z + \tfrac{4}{3} \tilde{u}_{zz} \tag{20}$$

$$\tilde{W}_t = (Pr \, Le)^{-1} \tilde{W}_{zz} \tag{21}$$

with boundary conditions at $z = 0$

$$\tilde{T} = H'(0)t \tag{22}$$

$$\tilde{W} = G'(1)H'(0)t - W_0 \tilde{\rho} \tag{23}$$

$$\tilde{u} = \frac{1}{Pr \, Le} \frac{\tilde{W}_z}{W_0 - 1} \tag{24}$$

and matching conditions for $z \to \infty$

$$\tilde{T} \to 0 \tag{25}$$

$$\tilde{W} \to 0. \tag{26}$$

The corresponding initial conditions are

$$\tilde{\rho} = \tilde{P} = \tilde{T} = \tilde{u} = 0, \quad \tilde{w} = 0 \quad \text{at} \quad t = 0. \tag{27}$$

The solution of equations (17)–(21) together with conditions (22)–(28) is expressed by

$$\tilde{W}(z, t) = 4\psi t i^2 \operatorname{erfc}\left(\frac{z\sqrt{(Pr \, Le)}}{2\sqrt{t}}\right) \tag{28}$$

where

$$\psi = G'(1)H'(0) - W_0 \frac{H'(0)(1 + \xi G'(1))}{\xi W_0 - 1}$$

$$\tilde{T}(z,t) = C_1 Ti^2 \operatorname{erfc}\left(\frac{z\sqrt{(Pr)}}{2\sqrt{t}}\right) + C_1' \tilde{W}(z,t). \tag{29}$$

Here

$$\xi = \frac{k_1}{k_1 W^0 + k_2}$$

$$C_1' = \frac{1}{Le-1}\frac{\gamma-1}{\gamma}\xi, \quad C_1 = 4[H'(0) - 4C_1']$$

$$\tilde{\rho}(z,t) = -C_1 ti^2 \operatorname{erfc}\left(\frac{z\sqrt{(Pr)}}{2\sqrt{t}}\right) - (C_1' + \xi)\tilde{W}(z,t) \tag{30}$$

$$\tilde{u}(z,t) = \sqrt{t}\left\{\overbrace{\frac{C_1}{2\sqrt{(Pr)}}\left[\pi^{-1/2} - i\operatorname{erfc}\left(\frac{z\sqrt{(Pr)}}{2\sqrt{t}}\right)\right]}^{\text{I}} + \overbrace{\frac{2(C_1' + \xi)}{\sqrt{(Le\ Pr)}}\left[\pi^{-1/2} - i\operatorname{erfc}\left(\frac{z\sqrt{(Le\ Pr)}}{2\sqrt{t}}\right)\right]}^{\text{II}} - \overbrace{\frac{2\psi}{\sqrt{\pi}(W_0 - 1)\sqrt{(Le\ Pr)}}}^{\text{III}}\right\} \tag{31}$$

$$\tilde{P}(z,t) = \tilde{P}_w(t) + \gamma\left\{\frac{(4Pr-3)}{12Pr}\left[C_1 \operatorname{erfc}\left(\frac{z\sqrt{(Pr)}}{2\sqrt{t}}\right) + \psi\frac{(C_1' + \xi)}{3}\operatorname{erfc}\left(\frac{z\sqrt{(Pr\ Le)}}{2\sqrt{t}}\right)\right] - \frac{z}{\sqrt{(\pi t)}}\left(\frac{C_1}{4Pr}\frac{(C_1' + \xi)}{\sqrt{(Pr\ Le)}}\psi - \frac{\sqrt{(Pr\ Le)}}{W_0 - 1}\psi\right)\right\} \tag{32}$$

in which $P_w(t)$ could be determined by a higher order approximation.

2.3.1.2. *The physics.* In equation (31), which gives the velocity in the boundary layer, the following terms can be identified:

term I represents the thermal expansion due to boundary heating;

term II represents the solutal expansion or contraction (depending on ξ, that is to say on the molar mass difference);

term III represents the mass flux at $x = 0$ due to the heterogeneous reaction.

At the edge of the boundary layer, the velocity $\tilde{u}$ is

$$\tilde{u} = \lim_{z\to\infty}\tilde{u}(z,t) = \left(\frac{C_1}{2\sqrt{(\pi\ Pr)}} + \frac{2(C_1' + \xi)}{\sqrt{(\pi\ Le\ Pr)}} - \frac{24}{\sqrt{(\pi\ Le\ Pr)}(W_0 - 1)}\right)\sqrt{t}. \tag{33}$$

The piston effect, already mentioned in ref. [3] is found again. The first term in equation (33) is the contribution of the thermal expansion, the second term is the contribution of the solutal expansion and the third term is the mass transfer at the wall. The boundary layer thickness increases as the square root of time.

In boundary condition (23) for the weight fraction $\tilde{W}(z,t)$ at $z = 0$, the first term represents the contribution of the increase in equilibrium partial specific mass ρ_A due to the increase in crystal temperature while the second term represents the contribution of the total specific mass. In other words, the first term only depends on thermodynamics (through the crystal temperature) and the second term depends on dynamical effects; this last term is the expression of the coupling between mechanical stresses and crystal growth, that is, possible mass transfer at the interface without any temperature variations at the surface.

As a matter of fact, the interface velocity given by boundary condition (7) for u and solution (28) for $\tilde{W}(z,t)$ is given as

$$\tilde{u}(0,t) = \left\{\overbrace{2[G'(1)H'(0)}^{\text{I}} - W_0\overbrace{\frac{H'(0)}{\xi W_0 - 1}}^{\text{II-1}}\overbrace{[1 + \xi G'(1)]}^{\text{II-2}}\right\} \times \frac{\sqrt{t}}{\sqrt{(\pi\ Le\ Pr)}(1 - W_0)}.$$

Term I is the contribution of the temperature dependent equilibrium partial specific mass ρ_A^s at the interface. Term II is the contribution of the total specific mass gradient at the interface ρ_x which undergoes variations under thermal (II-1) and solutal effects (II-2). Expression (34) for $\tilde{u}$ also points out that under linear increase of the interface temperature, the growth (or etching) varies as the square root of time.

2.3.2. *The core solution (outer solution)*

Expression (33) for the velocity at the edge of the initial boundary layer and the matching rule shows that

$$\lim_{x\to 0} u(x,t) = \lim_{t\to\infty}\tilde{u}(z,t) = \varepsilon^{3/2}\kappa\sqrt{t}$$

which means that a mechanical perturbation of the order of magnitude $O(\varepsilon^{3/2})$ acts on the bulk. On the other hand, taking form (32) $\lim_{t\to\infty}\tilde{P}(z,t)$, it becomes

$$\lim_{z\to\infty}\tilde{P}(z,t) = -\frac{\gamma}{\sqrt{(\pi t)}}\left(\frac{C_1}{4\sqrt{(Pr)}} + \frac{(C_1' + \xi)}{\sqrt{(Pr\ Le)}}\psi - \frac{\psi}{\sqrt{(Pr\ Le)}(W_0 - 1)}\right)z = \kappa' z = \varepsilon^{-1/2}\kappa' x$$

and

$$\lim_{z\to\infty} P(z,t) = 1 + \varepsilon^{-1/2}\kappa' x + O(\varepsilon)$$

matching conditions lead to

$$\lim_{x\to 0} P(x,t) = \lim_{z\to\infty} P(z,t) = 1 + \varepsilon^{3/2}\kappa' x + O(\varepsilon)$$

which means that the appropriate asymptotic expansions for the outer solution are

$$T(x,t) = 1+\varepsilon^{3/2}\bar{T}(x,t)+o(\varepsilon^{3/2}) \quad (34)$$

$$\rho(x,t) = 1+\varepsilon^{3/2}\bar{\rho}(x,t)+o(\varepsilon^{3/2}) \quad (35)$$

$$P(x,t) = 1+\varepsilon^{3/2}\bar{P}(x,t)+o(\varepsilon^{3/2}) \quad (36)$$

$$W(x,t) = 1+\varepsilon^{3/2}\bar{W}(x,t)+o(\varepsilon^{3/2}) \quad (37)$$

$$u(x,t) = \varepsilon^{3/2}\bar{u}(x,t)+o(\varepsilon^{3/2}). \quad (38)$$

Substituting equations (34)–(38) in equations (1)–(4), the following governing equations are obtained for the outer solution of $O(\varepsilon^{3/2})$:

$$\bar{\rho}_t+\bar{u}_x = 0 \quad (39)$$

$$\bar{u}_t+\gamma^{-1}\bar{P}_x = 0 \quad (40)$$

$$\bar{T}_t+(\gamma-1)\bar{u}_x = 0 \quad (41)$$

$$\bar{\rho}+\bar{T}+\xi\bar{W} = \bar{P} \quad (42)$$

$$\bar{W}_t = 0 \quad (43)$$

with initial conditions

$$\bar{u} = \bar{u}_t = 0, \quad \bar{W} = 0 \quad \text{at} \quad t = 0 \quad (44)$$

and boundary conditions:

at $x = 0$

$$\bar{u} = \kappa\sqrt{t}, \quad \bar{W} = 0, \quad T = 1+\varepsilon H'(0)t+o(\varepsilon); \quad (45)$$

and at $x = 1$

$$\bar{u} = 0, \quad \bar{W}_x = \bar{T}_x = 0. \quad (46)$$

The solution for $\bar{u}(x,t)$ is given by

$$\bar{u}_{tt} = \bar{u}_{xx} \quad (47)$$

and initial and boundary conditions (44)–(46). The Laplace transform technique leads to

$$\bar{u}(x,t) = \kappa(1-x)\sqrt{t}-\kappa\frac{\sqrt{2}}{\pi}\sum_{n=1}^{\infty}\frac{1}{n^{3/2}}\sin(n\pi x) \times[\cos\xi_n C_2(\xi_n)-\sin\xi_n S_2(\xi_n)] \quad (48)$$

where $\xi_n = n\pi t$ and obviously to

$$\bar{\rho}(x,t) = \tfrac{2}{3}\kappa t^{3/2}-\kappa\frac{\sqrt{2}}{\pi}\sum_{n=1}^{\infty}\frac{1}{n^{3/2}}\cos(n\pi x) \times[C_2(\xi_n)\sin\xi_n-S_2(\xi_n)\cos\xi_n] \quad (49)$$

$$\bar{T}(x,t) = (\gamma-1)\tfrac{2}{3}\kappa t^{3/2} -(\gamma-1)\kappa\frac{\sqrt{2}}{\pi}\sum_{n=1}^{\infty}\frac{1}{n^{3/2}}\cos(n\pi x) \times[C_2(\xi_n)\sin(\xi_n)-S_2(\xi_n)\cos\xi_n] \quad (50)$$

$$\bar{P}(x,t) = \gamma\left\{\tfrac{2}{3}\kappa t^{3/2}-\kappa\frac{\sqrt{2}}{\pi}\sum_{n=1}^{\infty}\frac{1}{n^{3/2}}\cos(n\pi x) \times[C_2(\xi_n)\sin\xi_n-S_2(\xi_n)\cos\xi_n]\right\}. \quad (51)$$

Here C_2 and S_2 represent the Fresnel integrals. Solutions (48)–(51) represent the isentropic propagation of an initial disturbance. It must be emphasized that solution (50) for T does not satisfy boundary conditions (45) at $x = 0.1$. This means that an adaptation layer exists near $x = 0.1$, and might be solved to reach a higher order approximation. On the other hand, solution (48) for u gives an increase without limit with time as $t \to \infty$ which means that for longer times this solution is no longer valid and that a multiple scale expansion technique must be used to reach the evolution on the long diffusion time scale.

2.4. *Description on the Long Diffusion Time Scale*

To reach the evolution on the diffusion time scale one must obtain the matching of the variable for $t \to \infty$.

One finds that in the limit $\varepsilon \to 0$, for x fixed and $\varepsilon t \ll 1$

$$u = \varepsilon\kappa(1-x)\sqrt{\sigma}+O(\tau) +\varepsilon^{3/2}\left\{-\kappa\frac{\sqrt{2}}{\pi}\sum_{n=1}^{\infty}G_n(x,t)+O(\sqrt{\tau})\right\}+O(\varepsilon^2) \quad (52)$$

$$\rho = 1+\tfrac{2}{3}\kappa\tau^{3/2}+O(\sigma^2) +\varepsilon^{3/2}\left\{-\kappa\frac{\sqrt{2}}{\pi}\sum_{n=1}^{\infty}G_n(x,t)+O(\sqrt{\tau})\right\}+O(\varepsilon^2) \quad (53)$$

$$P = 1+\tfrac{2}{3}\gamma\kappa\tau^{3/2}+O(\tau^2) +\varepsilon^{3/2}\left\{-\kappa\frac{\sqrt{2}}{\pi}\gamma\sum_{n=1}^{\infty}G_n(x,t)+O(\sqrt{\tau})\right\}+O(\varepsilon^2) \quad (54)$$

$$T = 1+\tfrac{2}{3}(\gamma-1)\kappa\tau^{3/2}+O(\tau^2) +\varepsilon^{3/2}\left\{-\kappa\frac{\sqrt{2}}{\pi}(\gamma-1)\sum_{n=1}^{\infty}G_n(x,t)+O(\sqrt{\tau})\right\}+O(\varepsilon^2). \quad (55)$$

Expansions (52)–(55) show that the $O(\varepsilon^{3/2})$ acoustic phenomena occurring on the t scale will continue to act on the $O(1)$ conduction controlled evolution occurring on the τ scale, and that the appropriate expansions are

$$\rho = \rho_d(\tau,x)+\varepsilon^{3/2}\rho_a(\tau,t,x)+O(\varepsilon^2)$$

$$P = P_d(\sigma,x)+\varepsilon^{3/2}P_a(\sigma,t,x)+O(\varepsilon^2)$$

$$T = T_d(\sigma,x)+\varepsilon^{3/2}T_a(\tau,t,x)+O(\varepsilon^2)$$

$$u = u_d(\tau,x)+\varepsilon^{3/2}u_a(\tau,t,x)+O(\varepsilon^2)$$

$$W = W_d(\tau,x)+O(\varepsilon).$$

Substituting these expansions into equations (1)–(4), the Navier–Stokes equations split into two systems. First the system giving the evolution on the τ scale

$$\rho_{d\tau}+(\rho_d u_d)_x = 0 \quad (56)$$

$$P_d = \rho_d\alpha_d T_d; \quad P_d \equiv P_d(\tau) \quad (57)$$

$$\frac{\rho_d}{\gamma-1}(T_{d\tau}+u_d T_{dx}) = -P_d u_{dx} + \frac{\gamma}{\gamma-1} Pr^{-1} T_{dxx} \quad (58)$$

$$W_{d\tau}+u_d W_{dx} = \frac{1}{Pr\,Le} W_{dxx} \quad (59)$$

with boundary conditions

$$T = H(\tau), \quad u = \frac{\varepsilon}{Pr\,Le}\frac{W_x}{\left(\frac{W^e(T)}{\rho}-1\right)},$$

$$W = W^e(T) \quad \text{at} \quad x = 0$$

$$T_x = 0, \quad u = 0, \quad W_x = 0 \quad \text{at} \quad x = 1$$

and initial conditions

$$P_d = \rho_d = T_d = 1, \quad u_d = 0 \quad \text{at} \quad \tau = 0$$

and the acoustic problem which is

$$\rho_{a\tau} + (\rho_d u_a)_x = 0 \quad (60)$$

$$\rho_d u_{a\tau} = -\frac{P_{ax}}{\gamma} \quad (61)$$

$$\rho_d(T_{a\tau}+u_d T_{ax}) = -(\gamma-1)P_d u_{ax} \quad (62)$$

$$W_{a\tau} = 0$$

with boundary conditions

$$T_a = u_a = 0 \quad \text{at} \quad x = 0, 1$$

and initial conditions

$$u_a = -\frac{\kappa}{2\pi}\sum_{n=1}^{\infty}\frac{1}{n^{3/2}}\sin(2\pi n x);$$

$$\rho_a = \frac{P_a}{\gamma} = \frac{T_a}{\gamma-1} - \frac{\kappa}{2\pi}\sum_{n=1}^{\infty} n^{-3/2}\cos(2\pi n x). \quad (63)$$

Equation (57) shows that the pressure is homogeneous on the diffusive scale: the acoustic wave has enough time to smooth out the pressure disturbance.

These two systems show that even on the long time scale compressibility effects should be taken into account.

3. THE NUMERICAL SOLUTION

3.1. *Principle of the Method*

The numerical method is based on a splitting technique and is called PISO for pressure implicit with splitting of operators [4]. The problem to solve is equations (1)–(4) with boundary conditions (5)–(8) and initial condition (8′).

The method consists first of solving equation (4) with an implicit $O(h^2)$ scheme, the other variables being fixed at the values they had at the previous time step n. Then, given $W^{n+1,1}(u^{n,1}, \rho^n)$ the velocity at time $(n+1)$ is computed from condition (7) for u. Given that condition for u and condition (5) for T, the Navier–Stokes equations are solved by the PISO technique and the solution used to reach the updated value

$$W^{n+1,l+1}(u^{n+1,l}, \rho^{n+1,l+1})$$

until convergence is reached, that is to say the full unsteady equations are solved at time step $(n+1)$.

The principle of the PISO algorithm already exposed in ref. [4] is briefly reported here.

3.1.1. *Principle of the PISO algorithm*

For each equation, one implicit predictor step is followed by n explicit corrector steps to take into account the variations of the other variables from one time step to another time step.

3.1.1.1. *Momentum predictor step.* This step consists of solving the implicit discretized equation

$$\left(\delta t^{-1} - \frac{A_0}{\rho^n}\right)\rho^n u_i^* = H(u_i^*) - \nabla_i P^n - \frac{\rho^n u_i^n}{\delta t} \quad (64)$$

which gives the provisional value u_i^*.

3.1.1.2. *First momentum corrector step.* The momentum equation is first written in the following form:

$$\left(\delta t^{-1} - \frac{A_0}{\rho^n}\right)\rho^* u_i^{**} = H(u_i^*) - \nabla_i P^* + \frac{\rho^n u_i^n}{\delta t}. \quad (65)$$

Subtracting equation (64) from equation (65) gives

$$\rho^* u_i^{**} - \rho^n u_i^* = -\left(\delta t^{-1} - \frac{A_0}{\rho^n}\right)^{-1}\nabla_i(P^* - P^n)$$

$$= -\left(\delta t^{-1} - \frac{A_0}{\rho^n}\right)^{-1}\nabla_i \bar{\bar{P}}. \quad (66)$$

If now the continuity equation is written as

$$\nabla_i(\rho^* u_i^{**}) = \delta t^{-1}(\rho^* - \rho^n) \quad (67)$$

taking the divergence of equation (66) and invoking equation (67) as well as the state equation written in the form

$$\rho^* = P^* \phi(W^n, T^n)$$

a Helmholtz equation is obtained for the pressure increment

$$\left\{\nabla_i\left[\left(\delta t^{-1} - \frac{A_0}{\rho^n}\right)^{-1}\nabla_i\right] - \frac{\phi(W^n, T^n)}{\delta t}\right\}\bar{\bar{P}}$$

$$= \nabla_i(\rho^n u_i^*) \quad (68)$$

and the boundary conditions are deduced from equation (66) written on the boundary point of a staggered grid for which the pressure and density are computed on external points and the other variables in inner points. This boundary condition is of the Robin type

$$\nabla_{1/2}\bar{\bar{P}} = u_{1/2}^{n+1}\phi_{1,2}^n \bar{\bar{P}}_{1,2}$$

where 1/2 identifies the boundary grid point. Equation (68) together with boundary conditions (70) give the first momentum corrector step, say u^{**} and P^*.

3.1.1.3. *Energy predictor step.* This implicit step solves the equation

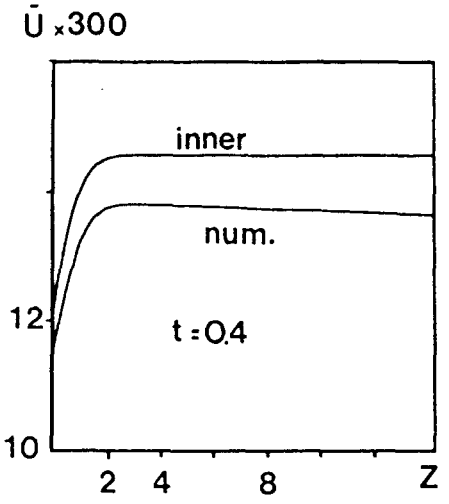

FIG. 2. Velocity in the initial boundary layer.

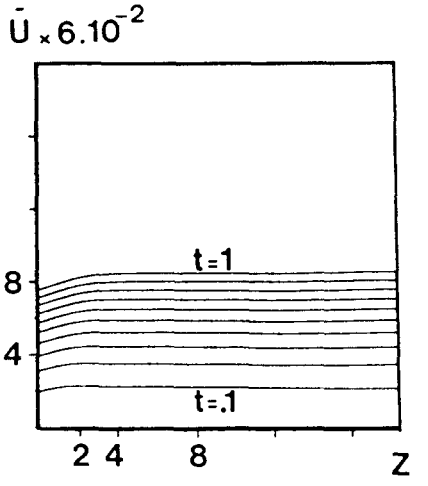

FIG. 3. Velocity in the boundary layer at various acoustic times.

$$\left(\delta t^{-1} - \frac{B_0}{\rho^*}\right)\rho^* e^* = G(e^*) - \nabla_i(\rho^* u_i^{**}) + J(u_i^{**}) + \frac{\rho^n u_i^n}{\delta t}.$$

After e^* has been obtained explicit momentum and energy corrector steps are performed until convergence. The precision of the method is $O(\delta t^n)$ where n is the number of corrector steps.

3.2. *Elements of Validation of the Method*

Comparison of numerical solution with asymptotic results is made in the case defined by boundary conditions (5)–(7), that is to say when the heat is added on the long diffusive time scale. The computation is performed for the following values of the physical parameters:

$$H'(0) = G'(1) = 1, \quad W_0 = 0.7,$$
$$\varepsilon = 4.77 \times 10^{-7}, \quad Pr = 0.76, \quad Pr\,Le = 1,$$
$$\gamma = 1.4, \quad \alpha = 1 \quad (M_A = M_B).$$

The numerical parameters are

$$\Delta x = 3.33 \times 10^{-4}, \quad \Delta t = 10^{-2}.$$

The corrector steps are stopped when $\Delta u/u$, $\Delta T/T$, $\Delta P/P$ are smaller than 10^{-2} and when $\Delta W/W < 10^{-8}$.

The computations are performed on a CYBER 990. The results for the velocity in the initial boundary layer are plotted on Fig. 2 as a function of the inner variable Z and for $t = 0.4$.

The comparison with the results for u computed from equation (31) evidence a 2% difference coming most probably from a loss of accuracy in the discretization of the concentration gradient when computing the boundary value for u from equation (7). The increase in velocity from its value at the wall due to the phase change and its asymptotic value when $z \to \infty$ comes from the expansion of the boundary layer adjacent to the wall under heating. It must be pointed out that the solutal effects are not taken into account since $\alpha = 1$. This behaviour could be different for other mass ratios of the diffusing species.

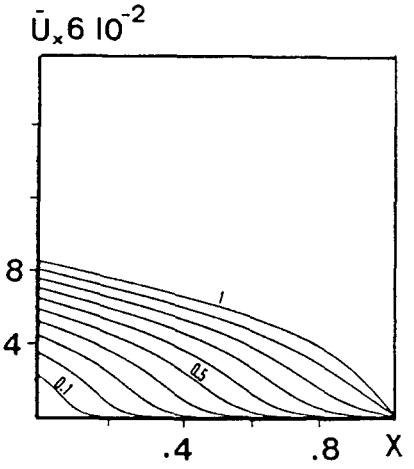

FIG. 4. Velocity in the core flow at various acoustic times.

3.3. *Solution for Typical Heating Law*

It is supposed that the relative increase in temperature is 10^{-2}, linearly, in 10^{-2} s, for $t \leqslant 30$

$$\varepsilon H'(0) = 3.33 \times 10^{-4}$$

in equations (5) and (6). Then, for $t > 0$, the temperature is constant. The parameters which differ form the set given in Section 3.2 are $M_B = 2M_A$ and $Pr\,Le = 1.52$.

3.3.1. *Solution on the acoustic scale*

3.3.1.1. *Boundary layer solution.* The velocity is plotted in Fig. 3 as a function of the inner variable z for $0 < t < 1$ with a 0.1 time step.

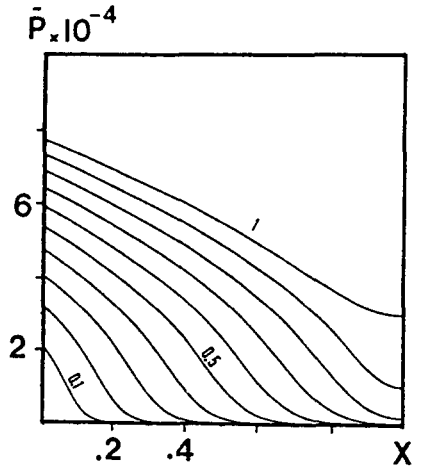

FIG. 5. Pressure in the core flow at various acoustic times.

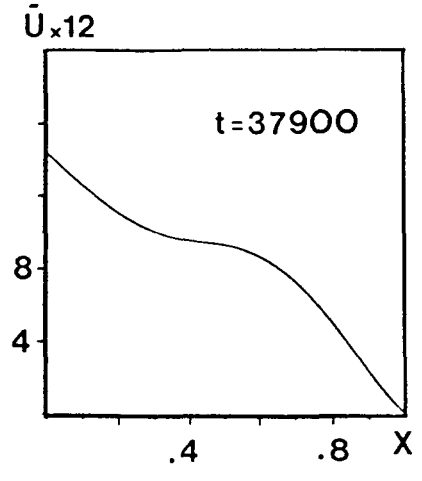

FIG. 6. Velocity in the core flow on the diffusion time scale.

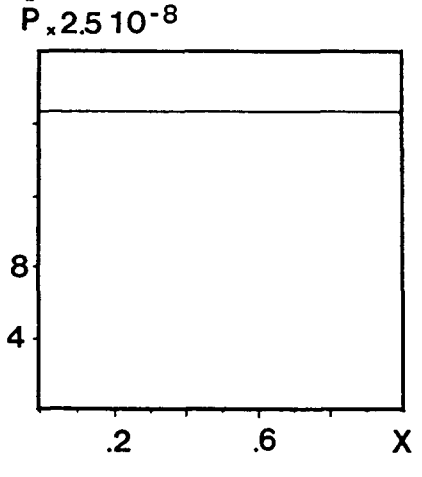

FIG. 7. Pressure in the core flow on the diffusive time scale.

The non-linear increase of the velocity at the interface must be pointed out and is due to the increase in equilibrium weight fraction.

3.3.1.2. *Core flow solution.* The velocity and pressure are plotted on Figs. 4 and 5 as a function of the outer variable x with a 0.1 time step. The propagation of the pressure wave at nearly sound velocity is shown. The pressure gradient is negative at $x = 0$ due to the mass flux and is zero at $x = 1$ because of the impermeability conditions.

3.3.2. *Solution on the diffusive scale*

The velocity and pressure in the core flow for $t = 37900$ are plotted on Figs. 6 and 7. The strong decrease of the velocity under stationary boundary conditions indicate that the new equilibrium is nearly reached. The plot of temperature and density would evidence quasi constant functions. The pressure is rigorously constant as predicted in Section 2.4, equation (58).

4. CONCLUSION

The present work has shown the efficiency of the PISO algorithm to solve low Mach number compressible flow. The comparison with asymptotic results gives a good agreement with analytical predictions. On a physical point of view the mechanisms of crystal sublimation have been analysed on both the acoustic and diffusive time scale. The analysis on the acoustic scale shows that the velocity in the initial, species and thermal, boundary layer is the result of two contributions: first the phase change which gives a non-zero velocity at the wall and then the expansion of the layer under thermal and solutal solicitations. On that short time scale there is no diffusion in acoustical isentropic bulk flow. Nevertheless this first application to the transient between two states of thermodynamic equilibrium between a crystal and its vapour has been chosen as an academic example. New applications of both asymptotic and numerical analysis are currently performed to study the influence of g-jitter or thermal disturbances on the transfer in the bulk and at the interface during crystal growth from the vapour phase.

REFERENCES

1. J. F. Clarke, D. R. Kassoy and N. Riley, Shock generated in a confined gas due to rapid heat addition at the boundary—I. Weak shock waves, *Proc. R. Soc. Lond.* **A393**, 309–329 (1984).
2. J. F. Clarke, D. R. Kassoy and N. Riley, Shock generated in a confined gas due to rapid heat addition at the boundary—II. Strong shock waves, *Proc. R. Soc. Lond.* **A393**, 331–351 (1984).
3. D. R. Kassoy, The response of a confined gas to a thermal disturbance—I. Slow boundary heating, *SIAM J. Appl. Math.* **36**(3) (June 1979).
4. R. I. Issa, Solution of the implicit discretized fluid flow equations by operator splitting, *J. Comp. Phys.* **62**(1), (January 1986).
5. B. Zappoli, Interaction between convection and surface reaction during *PVT* in closed ampoules, *J. Cryst. Growth* **76**, 449–461 (1986).

RESPONSE D'UNE INTERFACE DE CROISSANCE SOLIDE–GAZ A UNE AUGMENTATION DE TEMPERATURE

Résumé—La croissance cristalline à partir d'une phase vapeur et en ambiance de gravité réduite est étudiée à l'aide d'un problème—modèle mono-dimensionnel. Ce problème consiste à résoudre à l'aide de l'algorithme PISO les équations de transport relative à une espèce qui réagit à une interface pour explorer les transitoires entre deux états d'équilibre d'un cristal avec sa vapeur à deux températures différentes. Les équations du problème sont résolues par une méthode de développement asymptotiques raccordés, puis la comparaison avec les résultats numériques concernant l'évolution sur l'échelle de temps acoustique constitue une bonne validation de la solution numérique et des lois d'échelle.

VERHALTEN EINER WACHSENDEN PHASENGRENZFLÄCHE ZWISCHEN FESTEM UND GASFÖRMIGEM ZUSTAND BEI STEIGENDER TEMPERATUR

Zusammenfassung—Das instationäre Kristallwachstum aus der Dampfphase heraus wird mit einem eindimensionalen Modell für die Bedingungen der Mikrogravitation nachgebildet. Die Gleichungen für Kontinuität, Impuls-, Energie- und Stofftransport werden mit dem PISO-Algorithmus gelöst. Dabei wird eine Reaktion an der Grenzfläche berücksichtigt, die sich beim Übergang zwischen zwei Gleichgewichtszuständen des Kristalls und seiner dampfförmigen Umgebung infolge einer Temperaturänderung ergibt. Zusätzlich werden die grundlegenden Gleichungen mit Hilfe des Verfahrens der angepaßten asymptotischen Entwicklung gelöst. Ein Vergleich mit den numerischen Ergebnissen aus dem ersten Teil der Untersuchung führt zu einer guten Validierung des numerischen Verfahrens und der Skalierungsgesetze

ВЛИЯНИЕ УВЕЛИЧЕНИЯ ТЕМПЕРАТУРЫ НА РОСТ ГРАНИЦЫ РАЗДЕЛА ТВЕРДОЕ ТЕЛО–ГАЗ

Аннотация—С использованием одномерной модели исследуется нестационарный процесс роста кристалла из парообразной фазы в условиях микрогравитации. Данная модель включает численное решение уравнений неразрывности, импульса, энергии и переноса вещества, реагирующего у межфазной границы, с целью исследования переходного процесса между двумя состояниями равновесия кристалла и пара при двух различных температурах. Уравнения решались также методом сращивания асимптотических раздожений. Сравнение с численными результатами части I, рассматривающей эволюцию процесса в акустическом времени, подтвердило применимость предложенного численного метода и законов подобия.